

ChemComm

Chemical Communications

Accepted Manuscript

This article can be cited before page numbers have been issued, to do this please use: Y. Okazaki, S. Amimoto, K. Kozuka, S. Maekawa, K. Imato and Y. Ooyama, *Chem. Commun.*, 2026, DOI: 10.1039/D6CC01367H.



This is an Accepted Manuscript, which has been through the Royal Society of Chemistry peer review process and has been accepted for publication.

Accepted Manuscripts are published online shortly after acceptance, before technical editing, formatting and proof reading. Using this free service, authors can make their results available to the community, in citable form, before we publish the edited article. We will replace this Accepted Manuscript with the edited and formatted Advance Article as soon as it is available.

You can find more information about Accepted Manuscripts in the [Information for Authors](#).

Please note that technical editing may introduce minor changes to the text and/or graphics, which may alter content. The journal's standard [Terms & Conditions](#) and the [Ethical guidelines](#) still apply. In no event shall the Royal Society of Chemistry be held responsible for any errors or omissions in this Accepted Manuscript or any consequences arising from the use of any information it contains.

COMMUNICATION

Exploration of naphtho[*c*]dithiophenes: synthesis, optical and electrochemical properties of naphtho[1,2-*c*:5,6-*c'*]dithiophenes

Yuki Okazaki, Shogo Amimoto, Kumpei Kozuka, Satoru Maekawa, Keiichi Imato and Yousuke Ooyama*

Received 00th January 20xx,
Accepted 00th January 20xx

DOI: 10.1039/x0xx00000x

An efficient synthetic method for naphtho[1,2-*c*:5,6-*c'*]dithiophene and its tetrasubstituted derivative have been developed and their photophysical and electrochemical properties were revealed. The naphtho[*c*]dithiophene skeleton as a new thiophene-fused polycyclic aromatic systems would be used as a π -building blocks in the emitters, semiconductors and photosensitizers for organic optoelectronic devices.

Thiophene-fused polycyclic aromatic systems are of scientific and practical interest in synthetic organic chemistry, photochemistry and electrochemistry and as a key constituent of emitters, semiconductors and photosensitizers for organic optoelectronic devices.^{1–5} In particular, benzo[*b*]thiophenes and naphtho[*b*]dithiophenes, including naphtho[2,3-*b*:6,7-*b'*]dithiophene, naphtho[2,3-*b*:7,6-*b'*]dithiophene, naphtho[1,2-*b*:5,6-*b'*]dithiophene, and naphtho[2,1-*b*:6,5-*b'*]dithiophene, possessing high charge transport properties are widely used in organic field-effect transistors (OFETs), organic photovoltaics (OPVs), and organic light-emitting diodes (OLEDs) (Fig. 1a).^{6–15} Meanwhile, benzo[*c*]thiophenes, 1,1'- and 4,4'-bibenzo[*c*]thiophenes and fused- bibenzo[*c*]thiophenes have received considerable attention in recent years not only for a bold challenge to the development of facile and efficient synthetic methods, but also for their attractive photophysical and electrochemical properties to be promising fluorophore and photosensitizer for highly efficient bioimaging, phototheranostics, and optoelectronic devices (Fig. 1b).^{16–30}

Inspired by the strategic researches for the development and practical application of thiophene-fused polycyclic aromatic systems that will gain more and more extensive attention, we devised to construct naphtho[*c*]dithiophenes and to clarify their photophysical and electrochemical properties. Herein, we report an efficient synthetic method for naphtho[1,2-*c*:5,6-*c'*]dithiophene (**N[*c*]DT-1**) and its tetrasubstituted derivative (**N[*c*]DT-Si4**) with four *tert*-butyldimethylsilyl groups on two thiophene rings (Fig. 1c) and their photophysical and electrochemical properties based on photoabsorption and fluorescence spectroscopies, cyclic voltammetry (CV), and density functional theory (DFT) calculation. It was found

that **N[*c*]DT-1** possesses intense vibronic-structured photoabsorption and fluorescence bands in long-wavelength region and high HOMO energy level and low LUMO energy level, compared to its structural isomer naphtho[*b*]dithiophenes, naphtho[1,2-*b*:5,6-*b'*]dithiophene (**N[*b*]DT-3**) and naphtho[2,1-*b*:6,5-*b'*]dithiophene (**N[*b*]DT-4**) as well as isoelectronic chrysene with **N[*c*]DT-1**. Indeed, this work is the first to achieve the synthesis, photophysical and electrochemical characteristics of naphtho[*c*]dithiophenes.

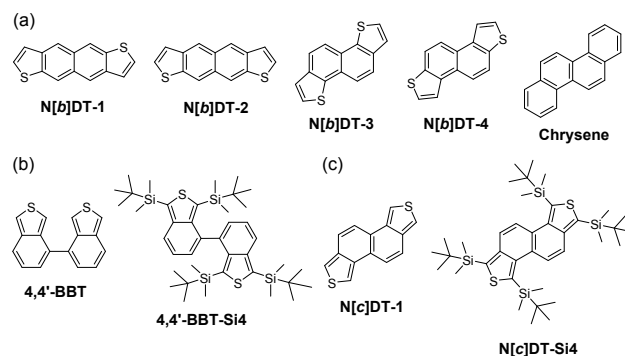


Fig. 1 (a) Chemical structures of naphtho[*b*]dithiophenes (Ref. 10) and chrysene. (b) Previous work (Ref. 25) for 4,4'-bibenzo[*c*]thiophenes and (c) this work for naphtho[*c*]dithiophenes.

N[*c*]DT-1 and its tetrasilyl-substituted derivative (**N[*c*]DT-Si4**) were synthesized according to a stepwise synthetic protocol (Scheme 1). The starting compound **1**, 1,2,5,6-tetramethylnaphthalene was prepared by the Wolff–Kishner reduction of 2,6-dimethylnaphthalene-1,5-dicarbaldehyde which was prepared by Bodroux–Chichibabin aldehyde synthesis using 1,5-dibromo-2,6-dimethylnaphthalene (Scheme S1, ESI†), because commercially available compound **1** is very expensive. The bromination of **1** with *N*-bromosuccinimide (NBS) gave compound **2** with a yield of 40%. Tetrahydronaphtho[1,2-*c*:5,6-*c'*]dithiophene **3** was obtained in a yield of 44% by the reaction of **2** with sodium sulfide. The oxidation of **3** with sodium periodate gave sulfoxide **4** with a moderate yield (59%) which is a key intermediate in the synthesis of naphtho[1,2-*c*:5,6-*c'*]dithiophenes. Indeed, naphtho[1,2-*c*:5,6-*c'*]dithiophene (**N[*c*]DT-1**) was successfully prepared in a yield of 53% or 30% by treatment of **4**

Applied Chemistry Program, Graduate School of Advanced Science and Engineering, Hiroshima University, 1-4-1 Kagamiyama, Higashi-Hiroshima 739-8527, Japan. E-mail: yooyama@hiroshima-u.ac.jp

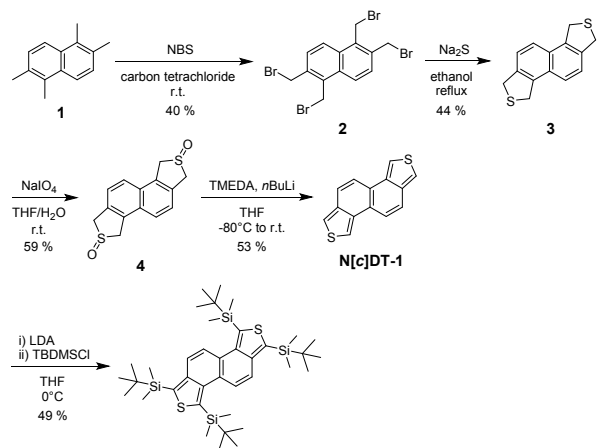
Electronic Supplementary Information (ESI) available. See DOI: 10.1039/x0xx00000x



COMMUNICATION

ChemComm

with tetramethylethylenediamine (TMEDA) and then *n*BuLi or with lithium hexamethyldisilazide (LHMDS) (see ESI†). Furthermore, the tetrasilyl-substituted derivative (**N[c]DT-Si4**) was obtained in a yield of 49% by the reaction of **N[c]DT-1** with lithium diisopropylamide (LDA), followed by treatment with *tert*-butyldimethylsilyl chloride (TBDMSCl) as an electrophile. The characterization of **N[c]DT-1** and **N[c]DT-Si4** was successfully determined by FTIR, ¹H and ¹³C NMR measurements and HRMS analysis. Therefore, this result proposes a facile and stepwise synthetic method for the introduction of various substituents, including bromo, stannyl, and boronic acid functional group for Stille or Suzuki coupling reaction, into the thiophene rings of naphtho[1,2-*c*:5,6-*c'*]dithiophene skeleton.



Scheme 1 Synthetic route to naphtho[1,2-*c*:5,6-*c'*]dithiophenes **N[c]DT-1** and **N[c]DT-Si4**.

The photoabsorption and fluorescence spectra of **N[c]DT-1** and **N[c]DT-Si4**, **4,4'-BBT** and **4,4'-BBT-Si4** as non-fused bibenzo[*c*]thiophenes, and isoelectronic chrysenes with **N[c]DT-1** in toluene are shown in Fig. 2, and their photophysical data along with those of **N[b]DT-3** and **N[b]DT-4** are summarized in Table 1. **N[c]DT-1** and **N[c]DT-Si4** exhibit vibronic-structured photoabsorption bands similar to **N[b]DT-3**, **N[b]DT-4** and chrysenes, although **4,4'-BBT** and **4,4'-BBT-Si4** exhibit broad photoabsorption bands. The photoabsorption maximum wavelength ($\lambda_{\max}^{\text{abs}} = 395$ nm) of **N[c]DT-1** showed bathochromic shifts by 36 nm, 75 nm, 45 nm and 73 nm, compared to those of **4,4'-BBT**, **N[b]DT-3**, **N[b]DT-4** and chrysenes, respectively. Furthermore, as with the case of **4,4'-BBT** and **4,4'-BBT-Si4**, **N[c]DT-Si4** exhibits an intense photoabsorption band ($\lambda_{\max}^{\text{abs}} = 411$ nm) with a relatively high molar absorption coefficient ($\epsilon_{\max} = 12\,700$ M⁻¹ cm⁻¹) in a longer wavelength region by 16 nm, compared to **N[c]DT-1** ($\epsilon_{\max} = 8600$ M⁻¹ cm⁻¹). The corresponding fluorescent band of **N[c]DT-1** has vibrational structure, as with that of chrysenes, although that of **N[c]DT-Si4** is broadened, as with those of **4,4'-BBT** and **4,4'-BBT-Si4** (Fig. 2). It is worth noting here that the fluorescence maximum wavelength ($\lambda_{\max}^{\text{fl}} = 407$ nm) of **N[c]DT-1** appeared in a shorter wavelength region by 38 nm, 3 nm and 44 nm, respectively, compared to those (445 nm, 410 nm and 451 nm, respectively) of **N[c]DT-Si4**, **4,4'-BBT** and **4,4'-BBT-Si4**. Thus, the Stokes shift (7.46×10^2 cm⁻¹) of **N[c]DT-1** is significantly smaller than those (1.85×10^3 cm⁻¹, 3.46×10^3 cm⁻¹, 4.78×10^3 cm⁻¹, and 3.43×10^3 cm⁻¹, respectively) of **N[c]DT-Si4**, **4,4'-BBT**, **4,4'-BBT-**

Si4, and chrysenes. Obviously, this result indicates that **N[c]DT-1** has rigid and expanded π -conjugation structure, compared to **4,4'-BBT**. Meanwhile, for **N[c]DT-Si4**, the broad fluorescence band and relatively large Stokes shift (SS) value is due to the rotatable and flexible *tert*-butyldimethylsilyl group. However, the fluorescence quantum yield ($\Phi_{\text{fl}} = 0.20$) of **N[c]DT-1** is higher than those (0.10) of **N[c]DT-Si4** and chrysenes, but is lower than those (0.41 and 0.36, respectively) of **4,4'-BBT** and **4,4'-BBT-Si4**. The time-resolved fluorescence spectroscopy demonstrated that the fluorescence lifetimes ($\tau_{\text{fl}} = 2.93$ ns and 1.00 ns) of **N[c]DT-1** and **N[c]DT-Si4** are a little shorter than those (3.46 ns and 3.59 ns) of **4,4'-BBT** and **4,4'-BBT-Si4**, but much shorter than that (12.1 ns) of chrysenes. The radiative rate constant ($k_{\text{r}} = 6.8 \times 10^7$ s⁻¹) for **N[c]DT-1** is about one-half those (1.0 – 1.1×10^8 s⁻¹) for **N[c]DT-Si4**, **4,4'-BBT** and **4,4'-BBT-Si4**, but the k_{r} value (8.2×10^6 s⁻¹) for chrysenes is much smaller than those for the other four compounds. In contrast, the nonradiative rate constant ($k_{\text{nr}} = 9.0 \times 10^8$ s⁻¹) for **N[c]DT-Si4** is significantly larger than those (7.4×10^7 – 2.7×10^8 s⁻¹) for the other four compounds. Thus, the ratio ($k_{\text{nr}}/k_{\text{r}} = 9.0$) of nonradiative constant to radiative constant for **N[c]DT-Si4** and chrysenes is larger than those (4.0, 1.5 and 1.7, respectively) for **N[c]DT-1**, **4,4'-BBT** and **4,4'-BBT-Si4**, indicating that the lower Φ_{fl} values of **N[c]DT-Si4** and chrysenes are mainly due to the larger k_{nr} value and smaller k_{r} value, respectively, compared to the Φ_{fl} values of **N[c]DT-Si4**, **4,4'-BBT** and **4,4'-BBT-Si4**. Consequently, these facts for naphtho[1,2-*c*:5,6-*c'*]dithiophene skeleton compared to 4,4'-bibenzo[*c*]thiophene skeleton, that is, the vibronic-structured photoabsorption and fluorescence bands in long-wavelength region, the mirror symmetry relationship, and the small Stokes shift value indicate that naphtho[*c*]dithiophene has rigid and expanded π -conjugation structure.

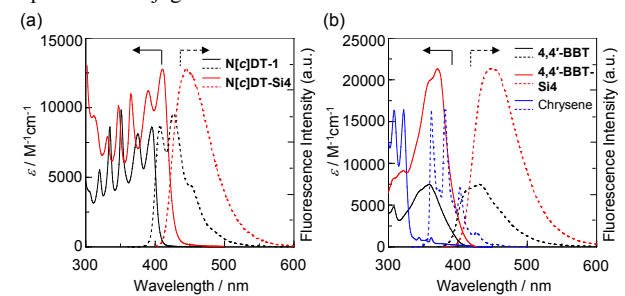


Fig. 2 Photoabsorption (solid line) and fluorescence (dotted line) spectra of (a) **N[c]DT-1** (1.0×10^{-4} M), **N[c]DT-Si4** (5.0×10^{-5} M), (b) **4,4'-BBT** (3.0×10^{-5} M), **4,4'-BBT-Si4** (3.0×10^{-5} M) and chrysenes (5.0×10^{-5} M) in toluene. Fluorescence intensity is normalized.

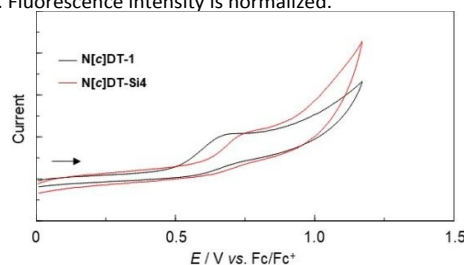


Fig. 3 Cyclic voltammograms of **N[c]DT-1** and **N[c]DT-Si4** in DMF containing 0.1 M Bu₄NClO₄ at a scan rate of 100 mV s⁻¹. The arrow denotes the direction of the potential scan.



Table 1 Photophysical and electrochemical data and HOMO and LUMO energy levels of naphtho[c]dithiophenes, 4,4'-bibenzo[c]thiophenes, naphtho[b]dithiophenes, and chrysene in the solution

Dye	$\lambda_{\text{max}}^{\text{abs}}/\text{nm}$ ($\epsilon_{\text{max}}/\text{M}^{-1}\text{cm}^{-1}$)	$\lambda_{\text{max}}^{\text{fl}}/\text{nm}$ (Φ_{fl}) ^f	SS/cm ⁻¹	$\tau_{\text{fl}}/\text{ns}$ ^g	$k_{\text{r}}/\text{s}^{-1}$ ^h	$k_{\text{nr}}/\text{s}^{-1}$ ⁱ	$k_{\text{nr}}/k_{\text{r}}$	$E_{\text{onset}}^{\text{ox}}/\text{V}$ ^j	$E_{\text{g}}^{\text{opt}}/\text{eV}$ ^k	HOMO/eV ^l	LUMO/eV ^l
N[c]DT-1	395 ^c (8600) ^a	407 ^d (0.20) ^a	7.46×10^2	2.93 ^a	6.8×10^{7a}	2.7×10^{8a}	4.0 ^a	0.50	3.10 ^a	-5.30	-2.20
N[c]DT-Si4	411 ^c (12 700) ^a	445 (0.10) ^a	1.85×10^3	1.00 ^a	1.0×10^{8a}	9.0×10^{8a}	9.0 ^a	0.59	2.94 ^a	-5.39	-2.45
4,4'-BBT ^m	359 (7500) ^a	410 (0.41) ^a	3.46×10^3	3.46 ^a	1.1×10^{8a}	1.7×10^{8a}	1.5 ^a	0.75 ^m	3.16 ^a	-5.55	-2.39
4,4'-BBT-Si4 ^m	371 (21 300) ^a	451 (0.36) ^a	4.78×10^3	3.59 ^a	1.0×10^{8a}	1.7×10^{8a}	1.7 ^a	0.54 ^m	3.04 ^a	-5.34	-2.30
N[b]DT-3 ⁿ	320 ^c (—) ^b	—	—	—	—	—	—	—	3.90 ^b	-5.80	-1.90
N[b]DT-4 ⁿ	350 ^c (—) ^b	—	—	—	—	—	—	—	3.50 ^b	-5.70	-2.20
Chrysene	322 ^c (16 400) ^a	362 ^d (0.10) ^a	3.43×10^3	12.1 ^a	8.2×10^{6a}	7.4×10^{7a}	9.0 ^a	1.00 ^p	3.71 ^a	-5.80	-2.09

^a In toluene. ^b In dichloromethane. ^c The longest wavelength maximum of vibronic-structured photoabsorption band. ^d The shortest wavelength maximum of vibronic-structured fluorescence band. ^e Photoabsorption edge. ^f Fluorescence quantum yields (Φ_{fl}) were determined by using a calibrated integrating sphere system ($\lambda^{\text{ex}} = 366 \text{ nm}$, 366 nm , 359 nm , 371 nm , and 318 nm for N[c]DT-1, N[c]DT-Si4, 4,4'-BBT, 4,4'-BBT-Si4, and chrysene, respectively). ^g Fluorescence lifetime. ^h Radiative rate constant ($k_{\text{r}} = \Phi_{\text{fl}}/\tau_{\text{fl}}$). ⁱ Nonradiative rate constant ($k_{\text{nr}} = (1 - \Phi_{\text{fl}})/\tau_{\text{fl}}$). ^j Onset potentials ($E_{\text{onset}}^{\text{ox}}$) versus Fc/Fc⁺ of the oxidation potential. ^k Optical energy gaps ($E_{\text{g}}^{\text{opt}}$) of N[c]DT-1, N[c]DT-Si4, 4,4'-BBT, and 4,4'-BBT-Si4 were determined from the intersection (400 nm, 422 nm, 393 nm, and 408 nm, respectively) of photoabsorption and fluorescence spectra in toluene. $E_{\text{g}}^{\text{opt}}$ of N[b]DT-3, N[b]DT-4, and chrysene were determined from photoabsorption edge (320 nm, 350 nm, and 334 nm, respectively). ^l Versus vacuum level. ^m Previous work (Ref. 25). ⁿ Ref. 10. ^o No data. ^p See Fig. S22 for cyclic voltammogram, †ESI.

The electrochemical properties of N[c]DT-1 and N[c]DT-Si4 were determined using CV in DMF containing 0.1 M tetrabutylammonium perchlorate (Bu_4NClO_4). The potentials were internally referenced to ferrocene/ferrocenium (Fc/Fc^+). The cyclic voltammograms of the two compounds are shown in Fig. 3, and their electrochemical data and the HOMO and LUMO energy levels are summarized in Table 1. The irreversible oxidation wave was observed at 0.68 V for N[c]DT-1 and 0.76 V for N[c]DT-Si4, while any obvious reduction wave did not appear within the potential window (-1.5 V – 0 V versus Fc/Fc^+). Thus, the oxidation wave for N[c]DT-1 is slightly cathodically shifted by ca. 0.10 V, compared to that for N[c]DT-Si4. The HOMO energy levels ($-[E_{\text{onset}}^{\text{ox}} + 4.8] \text{ eV}$) versus vacuum level were estimated from the onset potentials ($E_{\text{onset}}^{\text{ox}} = 0.50 \text{ V}$ for N[c]DT-1 and 0.59 V for N[c]DT-Si4) of the oxidation waves, and the LUMO energy levels were estimated from the $E_{\text{onset}}^{\text{ox}}$ and intersections (optical energy gap: $E_{\text{g}}^{\text{opt}} = 3.10 \text{ eV}$ for N[c]DT-1 and 2.94 eV for N[c]DT-Si4) of the photoabsorption and fluorescence spectra in toluene. The HOMO energy level (-5.30 eV) of N[c]DT-1 is significantly higher than those (-5.55 eV , -5.80 eV , -5.70 eV , and -5.80 eV) of 4,4'-BBT, N[b]DT-3, N[b]DT-4 and chrysene. Meanwhile, the LUMO energy level (-2.20 eV) of N[c]DT-1 is equivalent to that of N[b]DT-4, but is lower than those (-1.90 eV and -2.09 eV) of N[b]DT-3 and chrysene and is somewhat higher than that of (-2.39 eV) of 4,4'-BBT. Consequently, it was revealed that the bathochromic shift of the photoabsorption band for N[c]DT-1 relative to 4,4'-BBT, N[b]DT-3, N[b]DT-4 and chrysene is attributed to not only destabilization of the HOMO energy level and but also stabilization of LUMO energy level due to the naphtho[c]dithiophene skeleton, resulting in the decrease in the HOMO–LUMO band gap. Interestingly, the HOMO and LUMO energy levels of N[c]DT-Si4 are lower than those of N[c]DT-1, but the lowering of the LUMO energy level is larger than that of the HOMO energy level, whereas the HOMO and LUMO energy levels of 4,4'-BBT-Si4 are higher than those of 4,4'-BBT, but the rise of the HOMO energy level is larger than that of the LUMO energy level, resulting in the decrease in the HOMO–LUMO band gap, that is, the bathochromic shift of the photoabsorption band.

To examine the electronic structures of naphtho[1,2-c:5,6-c']dithiophenes, the molecular orbitals of N[c]DT-1 and N[c]DT-Si4 were calculated using DFT at the B3LYP/6-31G(d,p) level (Fig. 4). As with chrysene, the HOMO and the LUMO of N[c]DT-1 and

N[c]DT-Si4 are delocalized over the whole molecule. The DFT calculations demonstrated that the HOMO and LUMO energy levels of N[c]DT-1 are higher and lower than those of 4,4'-BBT, N[b]DT-3, N[b]DT-4 and chrysene, respectively, as with case of the experimental results, resulting in decrease in the HOMO–LUMO band gap. The fact that the HOMO–LUMO band gaps of N[b]DT-3, N[b]DT-4 and chrysene are wider than that of N[c]DT-1 can be understood from Clar's aromatic π -sextet rule, which states that the HOMO–LUMO band gap widens as the number of aromatic π -sextet in polycyclic aromatic hydrocarbon increases; N[b]DT-3, N[b]DT-4 and chrysene have four aromatic π -sextets, while N[c]DT-1 has two aromatic π -sextets.³¹ In addition, as with the case of 4,4'-BBT and 4,4'-BBT-Si4, the LUMO energy level of N[c]DT-Si4 is similar to that of N[c]DT-1, whereas the HOMO energy level of N[c]DT-Si4 is higher than that of N[c]DT-1, leading to the decrease in the HOMO–LUMO band gap. This result suggests that the destabilization of the HOMO energy level is due to the introduction of the electron-donating *tert*-butyldimethylsilyl group into the thiophene ring, although the change in the HOMO energy level from N[c]DT-1 to N[c]DT-Si4 by the DFT calculation is opposite to the experimental results. Furthermore, the time-dependent density functional theory (TD-DFT) calculations were performed to elucidate the photophysical properties of naphtho[1,2-c:5,6-c']dithiophenes (Fig. 5). The calculated $\lambda_{\text{max}}^{\text{abs-calc}}$ of the seven compounds appear in longer wavelength regions in the order of N[b]DT-3 (308 nm) < N[b]DT-4 (317 nm) \approx chrysene (322 nm) < 4,4'-BBT (345 nm) < 4,4'-BBT-Si4 (356 nm) < N[c]DT-1 (402 nm) < N[c]DT-Si4 (428 nm), and the calculated ϵ_{calc} increase in the order of N[c]DT-1 ($4200 \text{ M}^{-1} \text{ cm}^{-1}$) < chrysene ($5300 \text{ M}^{-1} \text{ cm}^{-1}$) < N[b]DT-3 ($6100 \text{ M}^{-1} \text{ cm}^{-1}$) < N[c]DT-Si4 ($6700 \text{ M}^{-1} \text{ cm}^{-1}$) < 4,4'-BBT ($7800 \text{ M}^{-1} \text{ cm}^{-1}$) < N[b]DT-4 ($12200 \text{ M}^{-1} \text{ cm}^{-1}$) < 4,4'-BBT-Si4 ($15600 \text{ M}^{-1} \text{ cm}^{-1}$). The $S_0 \rightarrow S_1$ transitions are mainly attributed to the transitions from the HOMO to the LUMO (99% for N[c]DT-1, 99% for N[c]DT-Si4, 67% for 4,4'-BBT, 68% for 4,4'-BBT-Si4, 55% for N[b]DT-3, and 89% for N[b]DT-4, 52% for chrysene). Indeed, the TD-DFT calculations are in good agreement with the experimental results about bathochromic shift of the photoabsorption band from N[b]DT-3 to N[c]DT-Si4, although there are difference in the ϵ_{calc} values between the experimental and TD-DFT calculation results.



COMMUNICATION

ChemComm

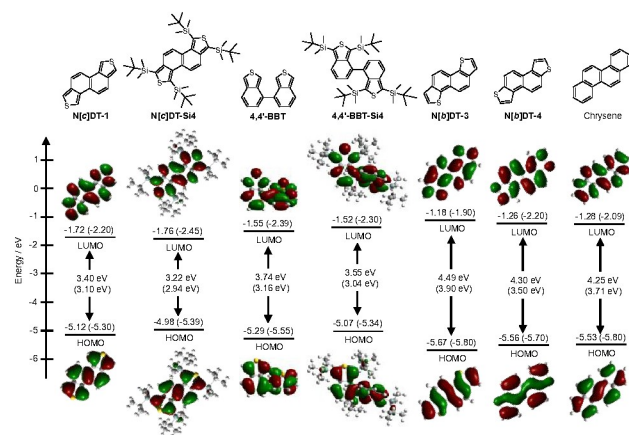


Fig. 4 Energy level diagram, HOMO and LUMO of N[c]DT-1, N[c]DT-Si4, 4,4'-BBT, 4,4'-BBT-Si4, N[b]DT-3, N[b]DT-4, and chrysenes derived from DFT calculations at the B3LYP/6-31G(d,p) level. Numbers in parentheses are the experimental values.

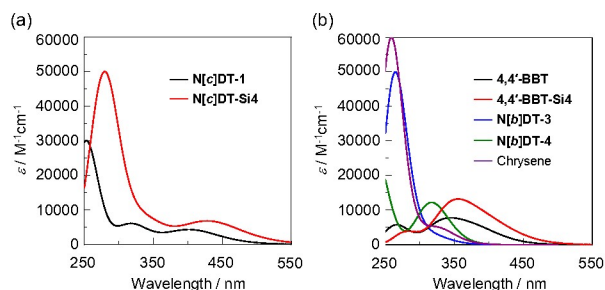


Fig. 5 Photoabsorption spectra of (a) N[c]DT-1, N[c]DT-Si4, (b) 4,4'-BBT, 4,4'-BBT-Si4, N[b]DT-3, N[b]DT-4, and chrysenes derived from TD-DFT calculations.

In conclusion, in order to construct naphtho[c]dithiophenes and to clarify their optical and electrochemical properties, we developed an efficient synthetic method for naphtho[1,2-c:5,6-c']dithiophene (N[c]DT-1) and its tetrasubstituted derivative (N[c]DT-Si4) with four *tert*-butyldimethylsilyl groups on two thiophene rings for the first time. Furthermore, this facile synthetic method will allow us to introduce various substituents, including bromo, stanny, and boronic acid functional group for Stille or Suzuki coupling reaction, into the thiophene rings of naphtho[1,2-c:5,6-c']dithiophene skeleton. The photophysical and electrochemical measurement, and density functional theory calculation revealed that naphtho[1,2-c:5,6-c']dithiophenes possess intense vibronic-structured photoabsorption and fluorescence bands in long-wavelength region and high HOMO energy level and low LUMO energy level, compared to its structural isomer naphtho[b]dithiophenes, naphtho[1,2-b:5,6-b']dithiophene and naphtho[2,1-b:6,5-b']dithiophene as well as isoelectronic chrysenes with naphtho[1,2-c:5,6-c']dithiophenes. Consequently, this work demonstrates that the naphtho[1,2-c:5,6-c']dithiophene skeleton with the above advantage properties would be used as a π -building blocks in the emitters, semiconductors and photosensitizers for organic optoelectronic devices, and thus will open up research and development of new thiophene-fused polycyclic aromatic systems.

Prof. Yousuke Ooyama conceived the project. Dr. Keiichi Imato directed the experimental work. Yuki Okazaki performed most of the experiments. Shogo Amimoto, Kumpei Kozuka, and Satoru Maekawa assisted with the experiment. The manuscript was written in contributions with all authors.

This work was supported by the Japan Society for the Promotion of Science (JSPS) KAKENHI Grant Number 25K01808 and 25K22857.

Conflicts of interest

The authors declare that there are no conflicts of interest.

Data availability

The data that support the findings of this work are available in supplementary information (SI). Supplementary Information: details of the experimental methods, additional figures and tables.

References

- L. Guo, L. Wu, T. Jia, H. Zhang, J. Song, X. Xie, M. H. Jee, H. Ma, S. Liu, G. Lu, H. Y. Woo, Z. Wang, F. Gao and Y. Sun *Angew. Chem. Int. Ed.*, 2025, **64**, e202516421.
- D. Zhang, X. Zheng, Y. Zhao, C. Zhao, F. Huang and Y. He, *J. Phys. Chem. C*, 2024, **128**, 7377–7387.
- D. Lee, J. Moon, S. Kim and J. Y. Lee, *Adv. Mater.*, 2026, e21668.
- E. B. A. Adusei, S. Ibrahim, K. Jenneker, C. D. Goldsmith, D. Dragoi, M. Zeller and Z. J. Kinney, *J. Org. Chem.*, 2026, **91**, 394–400.
- K. Kawabata, K. Mashimo and K. Takimiya, *Chem. Mater.*, 2024, **36**, 11920–11933.
- K. Haase, J. P. Andrade, M. Hamsch, V. Sethumadhavan, W. He, T. Michinobu, P. Sonar and S. C. B. Mannsfeld, *Adv. Electron. Mater.*, 2025, **11**, e00375.
- I. Osaka, T. Kakara, N. Takemura, T. Koganezawa and K. Takimiya, *J. Am. Chem. Soc.*, 2013, **135**, 8834–8837.
- I. Osaka, T. Abe, S. Shinamura and K. Takimiya, *J. Am. Chem. Soc.*, 2011, **133**, 6852–6860.
- S. Shinamura, E. Miyazaki and K. Takimiya, *J. Org. Chem.*, 2010, **75**, 1228–1234.
- S. Shinamura, I. Osaka, E. Miyazaki, A. Nakao, M. Yamagishi, J. Takeya and K. Takimiya, *J. Am. Chem. Soc.*, 2011, **133**, 5024–5035.
- M. E. Cinar and T. Ozturk, *Chem. Rev.*, 2015, **115**, 3036–3140.
- J. Y. Kim, D. Yokoyama and C. Adachi, *J. Phys. Chem. C*, 2012, **116**, 8699–8706.
- H. Usta, D. Kim, R. Ozdemir, Y. Zorlu, S. Kim, M. C. R. Delgado, A. Harbuzaru, S. Kim, G. Demirel, J. Hong, Y.-G. Ha, K. Cho, A. Facchetti and M.-G. Kim, *Chem. Mater.*, 2019, **31**, 5254–5263.
- H. Tan, H. Tan, X. Zheng, J. Yang, J. Yu and W. Zhu, *J. Mater. Chem. C*, 2020, **8**, 3183–3191.
- M. Liang and J. Chen, *Chem. Soc. Rev.*, 2013, **42**, 3453–3488.
- P. Amaladass, R. Dhanusuraman, A. Lazer, D. John, K. Thangaraju and V. Dhayalan, *Asian J. Org. Chem.*, 2025, **14**, e202500085.
- Y. Ooyama and K. Imato, *Tetrahedron Lett.*, 2025, **155**, 155393.
- K.-W. Lee, Y. Cao, W.-C. Wei, J.-H. Tan, Y. Wan, Z. Feng, Y. Zhang, Y. Liu, X. Zheng, C. Cao, H. Chen, P. Wang, S. Li, K.-T. Wong and C.-S. Lee, *Adv. Mater.*, 2023, **35**, 2211632.



- 19 D. Yan, M. Wang, Q. Wu, N. Niu, M. Li, R. Song, J. Rao, M. Kang, Z. Zhang, F. Zhou, D. Wang and B. Z. Tang, *Angew. Chem. Int. Ed.*, 2022, **61**, e202202614.
- 20 D. Yan, W. Xie, J. Zhang, L. Wang, D. Wang and B. Z. Tang, *Angew. Chem. Int. Ed.*, 2021, **60**, 26769–26776.
- 21 Y. Wan, G. Lu, W.-C. Wei, Y.-H. Huang, S. Le, J.-X. Chen, X. Cui, Y.-F. Xio, X. Li, Y. Liu, X.-M. Meng, P. Wang, H.-Y. Xie, J. Zhang, K.-T. Wong and C.-S. Lee, *ACS Nano*, 2020, **14**, 9917–9928.
- 22 X. Chen, D. Zhang, Y. He, M U. Ali, Y. Wu, C. Zhao, P. Wu, C. Yan, F. Wudl and H. Meng, *Mater. Chem. Front.*, 2020, **4**, 3578–3584.
- 23 K. Yamamoto, Y. Ie, M. Nitani, N. Tohnai, F. Kakiuchi, K. Zhang, W. Pisula, K. Asadi, P. W. M. Blom and Y. Aso, *J. Mater. Chem. C*, 2018, **6**, 7493–7500.
- 24 Y.-C. Hu, Z.-L. Lin, T.-C. Huang, J.-W. Lee, W.-C. Wei, T.-Y. Ko, C.-Y. Lo, D.-G. Chen, P.-T. Chou, W.-Y. Hung and K.-T. Wong, *Mater. Chem. Front.*, 2020, **4**, 2029–2039.
- 25 K. Obayashi, K. Imato, S. Aoyama, T. Enoki, S. Akiyama, M. Ishida, S. Suga, K. Mitsudo and Y. Ooyama, *RSC Adv.*, 2021, **11**, 18870–18880.
- 26 Y. Hara, K. Kozuka, K. Imato, S. Akiyama, M. Ishida and Y. Ooyama, *New J. Chem.*, 2024, **48**, 9890–9898.
- 27 T. Higashino, Y. Hara, K. Imato, S. Akiyama, M. Ishida and Y. Ooyama, *New J. Chem.*, 2023, **47**, 9555–9559.
- 28 K. Obayashi, S. Miho, M. Yasui, K. Imato, S. Akiyama, M. Ishida and Y. Ooyama, *New J. Chem.*, 2021, **45**, 17085–17094.
- 29 K. Obayashi, T. Higashino, K. Imato and Y. Ooyama, *New J. Chem.*, 2021, **45**, 13258–13261.
- 30 Y. Ooyama, T. Enoki, S. Aoyama and J. Ohshita, *Org. Biomol. Chem.*, 2017, **15**, 7302–7307.
- 31 E. Clar, *The Aromatic Sextet*, John Wiley & Sons, 1972.



Data availability

View Article Online
DOI: 10.1039/D6CC01367H

The data that support the findings of this work are available in supplementary information (SI).
Supplementary Information: details of the experimental methods, additional figures and tables.

